INTERNATIONAL JOURNAL FOR NUMERICAL METHODS IN FLUIDS, VOL. 7, 1053–1075 (1987)

ARBITRARY LAGRANGIAN–EULERIAN FINITE ELEMENT METHOD FOR UNSTEADY, CONVECTIVE, INCOMPRESSIBLE VISCOUS FREE SURFACE FLUID FLOW

BALASUBRAMANIAM RAMASWAMY* AND MUTSUTO KAWAHARA†

Department of Civil Engineering, Chuo University 13-27, Kasuga 1-Chome, Bunkyo-ku, Tokyo 112, Japan

SUMMARY

In this paper, free surface flow problems involving large free surface motions are analysed using finite element techniques. In solving these problems an arbitrary Lagrangian–Eulerian (ALE) kinematical description of the fluid domain is adopted, in which the nodal points can be displaced independently of the fluid motion. This formulation leads to an easy and accurate treatment of fluid–fluid interfaces, and greater distortions in the fluid motions can be handled than would be allowed by a purely Lagrangian method.

This paper describes the basic methodology, presents finite element approximations and discusses such matters as stability, accuracy and rezoning. The generality and the advantage of the present method are discussed, and its versatility is demonstrated through a few numerical experiments.

KEY WORDS ALE Method Incompressible Viscous Flow Velocity Correction Method Free Surface Linear Interpolation

INTRODUCTION

This paper presents the development of a new scheme to numerically simulate two-dimensional flow of an incompressible fluid with a free surface. Until very recently finite element solutions of unsteady, free surface flow invariably employed the Eulerian[1–10] or Lagrangian[11–15] descriptions of motion. Eulerian finite element calculations are characterized by a co-ordinate system that is stationary in the laboratory reference frame, so that fluid moves from element to element. The Eulerian method has several advantages: (a) the fluid can undergo arbitrarily great distortions without loss of accuracy, and (b) outflow 'walls' are particularly easy to handle. The difficulties encountered with basic Eulerian methodology are: (a) material interfaces lose their sharp definition as the fluid moves through the mesh, so that basic Eulerian calculations requires special logic for interfaces, which is very complicated, and often leads to inaccuracies, and (b) local regions of fine resolution are difficult to achieve. On the other hand, Lagrangian finite element calculations are characterized by a co-ordinate system that moves with the fluid. Accordingly, each computational element always contains the same fluid elements. The Lagrangian method has several useful and valuable properties: (a) material interfaces can be

Based on an invited lecture.
* Graduate Student
† Professor

0271–2091/87/101053–23$11.50

specifically delineated and precisely followed, (b) free surface boundary conditions are easily applied and (c) curved rigid boundaries of arbitrary shape can be present. The principal disadvantage is the inability to cope easily with strong distortions, which so often characterize flows of interest.

To circumvent the above-mentioned difficulties in both Eulerian and Lagrangian approaches, techniques have been proposed wherein the nodal points can be displaced independently of the fluid motion. The approach is described as an arbitrary Lagrangian–Eulerian (ALE) method, and is a combined Lagrangian and Eulerian computing method for fluid flow at all speeds based on Hirt's[16] findings with regard to the finite difference method and further refined by many others.[17–26] Because of the Lagrangian aspects of this technique it is applicable to flows with free surfaces, but it also maintains Eulerian aspects to overcome undesirable grid distortions often associated with Lagrangian methods. This technique is referred to as an arbitrary Lagrangian–Eulerian method because there are three options for moving vertices: (1) they can flow with the fluid for Lagrangian computing, (2) they can remain fixed for Eulerian computing or (3) they can move in an arbitrarily prescribed way to give a continuous rezoning capability.

The basic hydrodynamic part of each cycle of the ALE method is divided into three phases. The first phase is a typical, Lagrangian calculation. In the second phase, called the rezoning section, rezone velocities are specified to reduce distortions in the fluid domain. The third phase performs all the convective flux calculations, which must be included if the mesh is not purely Lagrangian. The purpose of using three phases is to know the Lagrangian motion before a choice is made for rezoning. This is the most general case. In some instances, however, the rezoning can be determined in advance and it is unnecessary to perform phase I and II calculations. For example, in a pure Eulerian calculation all vertices retain their initial positions. Conversely, if a pure Lagrangian calculation is desired, the phase II and III steps are unnecesssary since no rezoning is required. In practical applications, the hydrodynamics problem would be run for a while with the pure Lagrangian code and then stopped when the mesh begins to get somewhat distorted. The rezone code would then take over and smooth out the mesh, so that a desirable mesh configuration can be maintained. It should be noted that there is no time change during the rezoning operation. Then the mesh would be passed back to the hydrodynamics code for more time-dependent calculations. By this process of infrequent use of the rezoning, it is hoped that the mesh distortions may be held down enough to permit the problem to run satisfactorily.

KINEMATICS IN THE ALE DESCRIPTION

This section describes certain concepts, definitions and relations basic to the arbitrary Lagrangian–Eulerian description.

Co-ordinates

The material points of a continuous medium at time $t = 0$ occupy a region B, as shown in Figure 1. The position vector of a material point P in this region is given by

$$\mathbf{X} = (X_1, X_2, X_3). \tag{1}$$

The co-ordinates X_i are called material co-ordinates. In the deformed configuration the particle originally at P is located at the point p and has the position vector

$$\mathbf{x} = (x_1, x_2, x_3). \tag{2}$$

The co-ordinates x_i, which give the current position of the particle, are called spatial co-ordinates.

In the Lagrangian description the motion of the body carries various material particles through

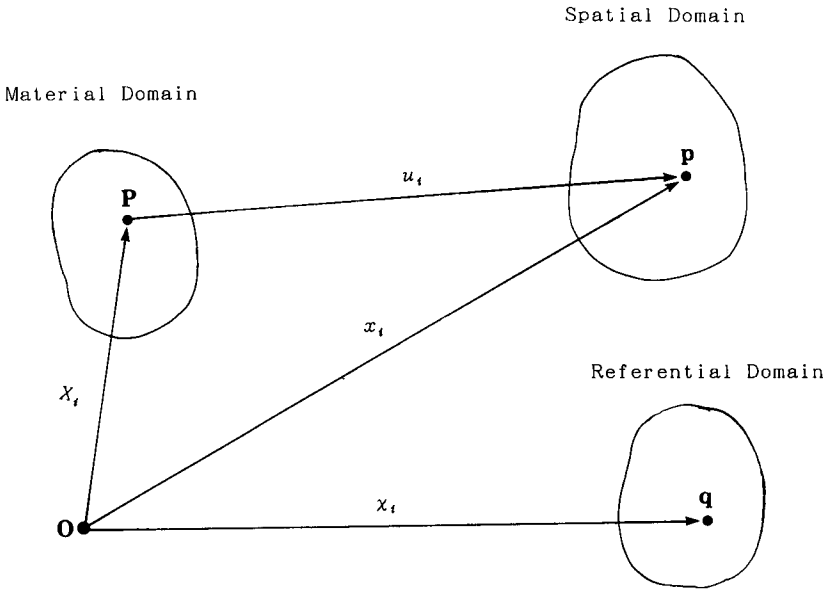

Figure 1. Co-ordinate system

various spatial positions. This idea is expressed mathematically by the relations

$$x_i = x_i(X_j, t). \tag{3}$$

These equations may be interpreted as a mapping of the initial configuration into the current configuration. For obvious reasons, the mappings (3) should be continuous, single-valued and possess a unique inverse for the Eulerian description as

$$X_i = X_i(x_j, t). \tag{4}$$

The necesssary and sufficient condition for the inverse functions (4) to exist is that the Jacobian determinant,

$$J = \det\left|\frac{\partial x_i}{\partial X_j}\right|, \tag{5}$$

should not vanish.

In addition to the spatial and material co-ordinates, a referential co-ordinate system is defined, as shown in Figure 1, which is independently prescribed as a function of space and time, by

$$\chi_i = \chi_i(x_j, t). \tag{6}$$

By analogy with equation (5) one defines the Jacobian,

$$\bar{J} = \det\left|\frac{\partial x_i}{\partial \chi_j}\right|, \tag{7}$$

for the transformation between referential and spatial co-ordinates.

Material derivatives of tensors: velocity and acceleration

In fluid mechanics, however, the rates of change of various kinematical quantities are generally more important than the quantities themselves. Let f be any physical quantity which is a

continuous function of the spatial variables x_i and time t, then in the case of the Lagrangian description the material derivative is defined by

$$f_{,t[X]} = \left.\frac{\partial f}{\partial t}\right|_{X_i}, \tag{8}$$

where the particle time derivative $\partial f/\partial t$ is taken with X_i held constant.

The spatial time derivative is given by

$$f_{,t[x]} = \left.\frac{\partial f}{\partial t}\right|_{x_i} \tag{9}$$

and the referential time derivative is

$$f_{,t[\chi]} = \left.\frac{\partial f}{\partial t}\right|_{\chi_i}. \tag{10}$$

The velocity of a material particle is given by

$$v_i = \left.\frac{\partial x_i}{\partial t}\right|_{X_i} \tag{11}$$

and the mesh velocity is defined as

$$w_i = \left.\frac{\partial x_i}{\partial t}\right|_{\chi_i}. \tag{12}$$

The difference of these two velocities is denoted by c_i:

$$c_i = v_i - w_i. \tag{13}$$

c_i is called the convective velocity in the mixed representation.

In the case of the ALE representation, the material time derivative is defined by

$$\frac{Df}{Dt} = \left.\frac{\partial f}{\partial t}\right|_{\chi_i} + \frac{\partial f}{\partial \chi_i}\frac{\partial \chi_i}{\partial t}. \tag{14}$$

Equation (11) can also be rewritten as

$$v_i = \frac{\partial x_i(\chi_j, t)}{\partial t} = \left.\frac{\partial x_i}{\partial t}\right|_{\chi_i} + \frac{\partial x_i}{\partial \chi_j}\frac{\partial \chi_j}{\partial t} \tag{15}$$

or

$$v_i = w_i + \frac{\partial x_i}{\partial \chi_j}\frac{\partial \chi_j}{\partial t}. \tag{16}$$

From equation (16) the following equation can be obtained:

$$\frac{\partial \chi_j}{\partial t} = (v_i - w_i)\frac{\partial \chi_j}{\partial x_i}. \tag{17}$$

Introducing equation (17) into equation (14) the following equation can be derived:

$$\frac{Df}{Dt} = \left.\frac{\partial f}{\partial t}\right|_{\chi_i} + \frac{\partial f}{\partial x_i}(v_i - w_i). \tag{18}$$

The acceleration components a_i in the case of the ALE description are given by

$$a_i = \left.\frac{\partial v_i}{\partial t}\right|_{\chi_i} + c_j v_{i,j}. \tag{19}$$

BASIC EQUATIONS FOR THE ALE DESCRIPTION

In this paper, the equations are described using indicial notation and the summation convention for repeated indices. The problem under consideration is the unsteady motion of a surface wave under gravity in a tank. Let V be the fluid domain, which is surrounded by a piecewise smooth boundary S. To illustrate the fluid-mechanical content of the formulation, the equations of conservation of momentum and mass for incompressible Newtonian fluids in the arbitrary Lagrangian–Eulerian form are given by the Navier–Stokes equation and the equation of continuity as follows:

$$\left.\frac{\partial v_i}{\partial t}\right|_{\chi_i} + c_j v_{i,j} - \sigma_{ij,j} = f_i, \quad \text{in} \quad V, \tag{20}$$

$$v_{i,i} = 0, \quad \text{in} \quad V. \tag{21}$$

Here $v_i = v_i(\chi, t)$ are the components of the velocity field in the mixed co-ordinate system $\chi_i (i = 1, 2)$ and $\mathbf{x}$ is used as shorthand for (χ_1, χ_2); $f_i (i = 1, 2)$ are the components of the gravitational acceleration and t is the time. The total stress tensor σ_{ij} is given by

$$\sigma_{ij} = -p\delta_{ij} + \nu(v_{i,j} + v_{j,i}), \tag{22}$$

where p is the pressure and ν is the coefficient of constant kinematic viscosity.

The boundary conditions for the ALE formulation are identical to those for the Eulerian or Lagrangian methods. In the present analysis, the boundary S consists of two kinds of boundaries, namely the free surface boundary S_1 and the solid wall boundary S_2 of the container. The conditions for velocity v_i and surface force t_i are introduced as follows:

$$v_i = \hat{v}_i, \quad \text{on} \quad S_2, \tag{23}$$

$$t_i = \{-p\delta_{ij} + \nu(v_{i,j} + v_{j,i})\} n_j = \hat{t}_i, \quad \text{on} \quad S_1, \tag{24}$$

where the superposed $\hat{}$ denotes the functions which are given on the boundary and n_j means the unit normal to the boundary. In the case of a free fluid boundary, the time evolution of the height function is governed by a kinematic equation expressing the fact that the free surface must move with the fluid,

$$\left.\frac{\partial \eta}{\partial t}\right|_{\chi_i} + (v_i^{(s)} - w_i^{(s)})\eta_{,i} = 0, \tag{25}$$

where η is the surface elevation measured from the fundamental fluid level and $v_i^{(s)}$ and $w_i^{(s)}$ are the x_i-components of the fluid particle velocity and mesh velocity at the nodal points of the free surface.

The initial conditions for Navier–Stokes problem (20)–(22) consist of specifying the values of velocity and pressure at the initial time:

$$v_i(x_i, 0) = v_i^{(0)}(x_i), \tag{26}$$

$$p(x_i, 0) = p^{(0)}(x_i), \tag{27}$$

with the initial velocity $v_i^{(0)}(x_i)$ satisfying the incompressibility condition:

$$v_{i,i}^{(0)} = 0. \tag{28}$$

WEIGHTED RESIDUAL FORMULATIONS

A week formulation of problem (20)–(28) is obtained by multiplying the differential equations by suitable weighting functions and integrating over a domain $V(\chi_i, t)$, which is bounded by a surface S with a unit normal n_i. Next, multiply the momentum equation (20) by the weighting function v_i^*, and the continuity equation (21) by the weighting function q^*, and then integrate over V. After integration by parts of the stress term, use of the divergence theorem and of the boundary condition (24), the following weak form of the original problem is obtained:

$$\int_V \left(v_i^* \frac{\partial v_i}{\partial t} \right) \mathrm{d}V = - \int_V (v_i^* c_j v_{i,j}) \, \mathrm{d}V + \int_V (v_{i,i}^* p) \, \mathrm{d}V - \nu \int_V \{ v_{i,j}^* (v_{i,j} + v_{j,i}) \} \, \mathrm{d}V + \int_V (v_i^* f_i) \, \mathrm{d}V + \int_S [v_i^* \{ -p\delta_{ij} + \nu(v_{i,j} + v_{j,i}) \} n_j] \, \mathrm{d}S, \tag{29}$$

$$\int_V (q^* v_{i,i}) \, \mathrm{d}V = 0, \tag{30}$$

with

$$v_i = \hat{v}_i, \quad \text{on} \quad S_1, \tag{31}$$

$$v_i(x_i, 0) = v_i^{(0)}(x_i). \tag{32}$$

In a similar fashion, the weak form for equation (25) can be obtained by multiplying by the weighting function η^* as

$$\int_V \left(\eta^* \frac{\partial \eta}{\partial t} \right) \mathrm{d}V + \int_V (\eta^* c_i^{(s)} \eta_{,i}) \, \mathrm{d}V = 0. \tag{33}$$

Under suitable smoothness conditions for the boundary date $\hat{v}_i$ and $\hat{t}_i$, the Navier–Stokes problem (29)–(33) admits at least one solution.

TIME DISCRETIZATION

In order to implement a numerical solution procedure for the arbitrary Lagrangian–Eulerian formulation in this paper, the momentum equation and the incompressibility constraint of the Navier–Stokes problem are treated according to a procedure consisting of three phases. Let v_i^n and p^n be the velocity and pressure fields at time t^n, where $t^n = t^{n+1} + \Delta t$. From v_i^n, p^n and the boundary specifications, the fields v_i^{n+1} and p^{n+1} are calculated as follows.

Phase I: Lagrangian calculations

Phase I is governed by the Lagrangian equations obtained from equations (29)–(33) by setting c_j to zero in equations (29) and (33). In this phase the material acceleration can be approximated by the increment of the velocity in the following form:

$$\left. \frac{\partial v_i}{\partial t} \right|_{x_i} \doteqdot \frac{(v_i^{\mathrm{L}} - v_i^n)}{\Delta t}, \tag{34}$$

where the velocities and positions of each fluid particle $P_K = P_K(x_i^0, t_0)$ with the initial location x_i^0

at time t^0 are defined by

$$v_i^n = v_i(P_K, t^n), \tag{35a}$$

$$x_i^n = x_i(P_K, t^n), \tag{35b}$$

and

$$v_i^L = v_i(P_K, t^{n+1}), \tag{36a}$$

$$x_i^L = x_i(P_K, t^{n+1}). \tag{36b}$$

At first, an intermediate velocity field $\tilde{v}_i^L$, not satisfying the incompressibility constraint, is derived from a time-discretized version of the weak form of the momentum equation in which the pressure terms are omitted. Then, the field $\tilde{v}_i^L$ is decomposed into the sum of a vector field with zero divergence and a vector field with zero curl. The divergenceless component is the end-of-step Lagrangian velocity vector v_i^L, whereas the irrotational one is related to the gradient of the pressure field p^L.

The intermediate Lagrangian nodal velocity field $\tilde{v}_i^L$, not satisfying the incompressibility condition, is derived from the previous cycle's velocity vectors, position vectors and body forces by employing the purely explicit Euler first-order scheme:

$$\begin{aligned}\int_{V^L} (v_i^* \tilde{v}_i^L)\,\mathrm{d}V = \int_{V^n} (v_i^* v_i^n)\,\mathrm{d}V - \Delta t\Bigg[& \int_{V^n} (v_i^* f_i)\,\mathrm{d}V \\ & + \nu\left\{ \int_{V^n} (v_{i,j}^* v_{i,j}^n)\,\mathrm{d}V + \int_{V^n} (v_{i,j}^* v_{j,i}^n)\,\mathrm{d}V \right\} \\ & - \nu\left\{ \int_{S^n} (v_i^* v_{i,j}^n + v_i^* v_{j,i}^n) n_j\,\mathrm{d}S \right\} \Bigg],\end{aligned} \tag{37}$$

$$\tilde{u}_i^L = \hat{v}_i, \quad \text{on} \quad S_2. \tag{38}$$

Once the intermediate velocity has been computed, the end-of-step velocity v_i^L is obtained by adding to $\tilde{v}_i^L$ the dynamical effect of the still-unknown pressure p^L, which is to be determined so that the weak form (30) of the incompressibility condition remains satisfied:

$$\int_{V^L} (v_i^* v_i^L)\,\mathrm{d}V = \int_{V^L} (v_i^* \tilde{v}_i^L)\,\mathrm{d}V - \Delta t \int_{V^L} (v_i^* p_{,i}^L)\,\mathrm{d}V, \tag{39}$$

$$\int_{V^L} (q^* v_{i,i}^L)\,\mathrm{d}V = 0. \tag{40}$$

Perhaps the most important feature of the current formulation, compared to previous finite element methods, is the pressure solution approach. The current formulation is an iterative, segregated solution method along the lines of most finite difference methods. Morever, the present formulation uses an equal order interpolation approximation for velocity and pressure rather than a mixed order approximation. The use of an equal order approximation for pressure represents a significant departure from the use of a mixed order approximation, which has been advocated by numerous researchers. An equal order approximation may be used if the formulation includes a Poisson type of equation to solve for pressure. However, there are several difficulties associated with the use of a Poisson pressure equation which must be overcome. First of all, a conventional Poisson pressure equation[27] imparts no direct continuity constraint, and as a result may provide very poor convergence. Secondly, specification of the boundary conditions for the pressure equation is not straightforward with the conventional form of the Poisson pressure equation. As will be shown, the current approach does not suffer from these difficulties.

Using the concept of divergence on both sides of equation (39) together with the incompressibility constraint $v^{\mathrm{L}}_{i,i} = 0$, the following linear system of equations, which governs the pressure field, can be derived:

$$\int_{V^{\mathrm{L}}} (q^* p^{\mathrm{L}}_{,ii})\,\mathrm{d}V = \frac{1}{\Delta t}\int_{V^{\mathrm{L}}} (q^* \tilde{v}^{\mathrm{L}}_{i,i})\,\mathrm{d}V. \tag{41}$$

The left-hand side of equation (41) contains derivatives of second order which may be reduced to first order through an integration by parts. Equation (41) is then

$$\int_{V^{\mathrm{L}}} (q^*_{,i} p^{\mathrm{L}}_{,i})\,\mathrm{d}V = -\frac{1}{\Delta t}\int_{V^{\mathrm{L}}} (q^* \tilde{v}^{\mathrm{L}}_{i,i})\,\mathrm{d}V = \int_{S^{\mathrm{L}}} (q^* p^{\mathrm{L}}_{,i} n_i)\,\mathrm{d}S, \tag{42}$$

where the divergence theorem has been used to obtain the boundary integral. To solve the above equation (42), the following boundary conditions are applied:

$$p^{\mathrm{L}} = 0, \quad \text{on} \quad S_1, \tag{43}$$

$$p^{\mathrm{L}}_{,i} n_i = 0, \quad \text{on} \quad S_2. \tag{44}$$

Once the pressure has been determined from equation (42), Lagrangian velocities are calculated from equation (39). Finally, the vertex co-ordinates at the end of the Lagrangian phase are calculated by

$$x^{\mathrm{L}}_i \doteq x^n_i + \frac{\Delta t}{2}(v^{\mathrm{L}}_i + v^n_i). \tag{45}$$

If only a Lagrangian calculation is wanted then vertices are moved according to equation (45) and the procedure of the phase I calculation can be repeated for more time-dependent calculations. Otherwise, rezone velocities must be specified and phase II and III calculations must be performed.

Phase II: the rezone velocity

As is well known, in computational fluid dynamics there is often the need to change the computational mesh. This may occur, for example, in Lagrangian calculations when the mesh becomes severely distorted, or in an adaptive mesh algorithm when the mesh is changed to satisfy various criteria. When this happens there is a need to transfer information from the old mesh to the new mesh. This transfer of information is an interpolation process which is frequently called rezoning (or remapping). Such an interpolation process may be quite arbitrary, but the present study is interested in imposing one important restriction, namely that the process should be conservative. The conservation equations of fluid dynamics express the fact that certain conserved quantities, such as mass, momentum and total energy, are neither created nor destroyed. These requirements are clearly satisfied in the next phase by computing the necessary rezoning changes, i.e. convective and diffusive fluxes.

Assume at this point that a field of mesh vertex velocities, w_i has been assigned in some appropriate fashion with respect to a fixed, Eulerian reference frame. Thus, for a purely Eulerian calculation.

$$w_i = 0 \tag{46}$$

At the other extreme, a purely Lagrangian calculation would use

$$v_i = w_i. \tag{47}$$

In general, the mesh velocities may be any designated functions, and as such they are neither purely Eulerian nor purely Lagrangian. Once the rezone or mesh velocities are assigned, vertices are moved according to the prescription

$$x_i^{n+1} = x_i^n + \Delta t w_i. \tag{48}$$

From these values new element volumes and masses can be computed.

Phase III: convective flux calculations

There are two types of quantities to be updated in the rezone: element quantities, namely the mass or volume, and vertex quantities, namely the velocity components v_i and the pressure field p. Using equation (48) new element volumes and masses can be computed. It now remains to describe the calculations that account for the transfer of mass and momentum between elements during rezoning. A temporary velocity field is first calculated that accounts for the convective fluxes:

$$\int_{V^{n+1}} (v_i^* \tilde{v}_i^{n+1})\,\mathrm{d}V = \int_{V^L} (v_i^* \tilde{v}_i^L)\,\mathrm{d}V + \Delta t \int_{V^n} (v_i^* c_j v_{i,j}^n)\,\mathrm{d}V, \tag{49}$$

$$\tilde{v}_i^{n+1} = \hat{v}_i, \quad \text{on} \quad S_2. \tag{50}$$

Final velocities for the cycle are obtained by combining the temporary velocities $\tilde{v}_i^{n+1}$ with the pressure acceleration in the following manner:

$$\int_{V^{n+1}} (v_i^* v_i^{n+1})\,\mathrm{d}V = \int_{V^{n+1}} (v_i^* \tilde{v}_i^{n+1})\,\mathrm{d}V - \Delta t \int_{V^{n+1}} (v_i^* p_{,i}^{n+1})\,\mathrm{d}V, \tag{51}$$

$$\int_{V^{n+1}} (q^* v_{i,i}^{n+1})\,\mathrm{d}V = 0. \tag{52}$$

The pressure needed in equation (51) is that which ensures satisfaction of the incompressibility condition. That is, the final velocity field must possess a zero velocity divergence in every element, as described in equation (52). This is accomplished by solving the equation which governs the pressure field:

$$\int_{V^{n+1}} (q^* p_{,ii}^{n+1})\,\mathrm{d}V = \frac{1}{\Delta t} \int_{V^{n+1}} (q^* \tilde{v}_{i,i}^{n+1})\,\mathrm{d}V. \tag{53}$$

The left-hand side of equation (53) contains derivatives of second order which may be reduced to first order through an integration by parts. Equation (53) is then

$$\int_{V^{n+1}} (q_{,i}^* p_{,i}^{n+1})\,\mathrm{d}V = -\frac{1}{\Delta t} \int_{V^{n+1}} (q^* \tilde{v}_{i,i}^{n+1})\,\mathrm{d}V + \int_{S^{n+1}} (q^* p_{,i}^{n+1} n_i)\,\mathrm{d}S, \tag{54}$$

where the divergence theorem has been used to obtain the boundary integral. To solve equation (54), the following boundary conditions are applied:

$$p^{n+1} = 0, \quad \text{on} \quad S_1, \tag{55}$$

$$p_{,i}^{n+1} n_i = 0, \quad \text{on} \quad S_2. \tag{56}$$

Equation (54) is a symmetric system of linear algebraic equations which may be solved via a direct method, such as the skyline version of Gaussian elimination. Once the pressure has been obtained, the end-of-step velocity is computed from equation (51).

The position of the free surface is calculated from the following equation:

$$\int_{V^{n+1}} (\eta^* \eta^{n+1})\,\mathrm{d}V = \int_{V^{\mathrm{L}}} (\eta^* \eta^{\mathrm{L}})\,\mathrm{d}V - \Delta t \int_{V^n} (\eta^* c_i^{(\mathrm{S})} \eta_{,i}^n)\,\mathrm{d}V. \tag{57}$$

This completes the updating of all quantities.

FINITE ELEMENT METHOD

The full discrete form of the problems (37)–(44) and (49)–(57) is obtained by discretizing the domain V into non-overlapping subregions called finite elements. In each element the unknowns fields are approximated by simple polynomial functions. For the present class of problems let the velocity and pressure be represented within an element by

$$v_i = \Phi_\alpha v_{\alpha i}, \tag{58}$$

$$p = \Phi_\alpha p_\alpha, \tag{59}$$

$$\eta = \Phi_\alpha \eta_\alpha, \tag{60}$$

and the corresponding weighting functions are

$$v_i^* = \Phi_\alpha v_{\alpha i}^*, \tag{61}$$

$$p^* = \Phi_\alpha p_\alpha^*, \tag{62}$$

$$\eta^* = \Phi_\alpha \eta_\alpha^*, \tag{63}$$

where Φ_α is the interpolation function, $v_{\alpha i}$ represents the nodal value of the velocity at the αth node of the finite element in the ith direction and $v_{\alpha i}^*$ is the nodal value of the corresponding weighting function. p_α is the nodal value for pressure at αth node of the finite element and p_α^* is the nodal value of the corresponding weighting function. Substituting equations (58)–(63) into (37), (39), (42), (49), (51) and (54), and considering the arbitrariness of the weighting functions, the finite element equations for phase I and phase III can be derived as follows.

For phase I

$$\bar{M}_{\alpha\beta}^{\mathrm{L}} \bar{v}_{\beta i}^{\mathrm{L}} = \bar{M}_{\alpha\beta}^n v_{\beta i}^n - \Delta t (S_{\alpha i \beta j}^n v_{\beta j}^n - N_\alpha^n f_{\alpha i}^n - \hat{\Omega}_{\alpha i}^n), \tag{64}$$

$$\bar{M}_{\alpha\beta}^{\mathrm{L}} v_{\beta i}^{\mathrm{L}} = \bar{M}_{\alpha\beta}^{\mathrm{L}} \bar{v}_{\beta i}^{\mathrm{L}} - \Delta t H_{\alpha i \beta}^{\mathrm{L}} p_\beta^{\mathrm{L}}, \tag{65}$$

$$A_{\alpha\beta}^{\mathrm{L}} p_\beta^{\mathrm{L}} = -\left(\frac{1}{\Delta t}\right) H_{\alpha i \beta}^{\mathrm{L}} \bar{v}_{\beta i}^{\mathrm{L}} + \hat{\Sigma}_\alpha^{\mathrm{L}}. \tag{66}$$

For phase III

$$\bar{M}_{\alpha\beta}^{n+1} \bar{v}_{\beta i}^{n+1} = \bar{M}_{\alpha\beta}^{\mathrm{L}} \bar{V}_{\beta i}^{\mathrm{L}} - \Delta t K_{\alpha\beta\gamma j}^n c_{\beta j}^n v_{\gamma i}^n, \tag{67}$$

$$\bar{M}_{\alpha\beta}^{n+1} v_{\beta i}^{n+1} = \bar{M}_{\alpha\beta}^{n+1} \bar{v}_{\beta i}^{n+1} - \Delta t H_{\alpha i \beta}^{n+1} p_\beta^{n+1}, \tag{68}$$

$$A_{\alpha\beta}^{n+1} p_\beta^{n+1} = -\left(\frac{1}{\Delta t}\right) H_{\alpha i \beta}^{n+1} \bar{v}_{\beta i}^{n+1} + \hat{\Sigma}_\alpha^{n+1}, \tag{69}$$

$$\bar{M}_{\alpha\beta}^{n+1} \eta_\beta^{n+1} = \bar{M}_{\alpha\beta}^{\mathrm{L}} \eta_\beta^{\mathrm{L}} - \Delta t K_{\alpha\beta\gamma i}^n c_{\beta j}^n \eta_\gamma^n, \tag{70}$$

where

$$M^n_{\alpha\beta} = \int_{V^n} (\Phi^n_\alpha \Phi^n_\beta)\,\mathrm{d}V,$$

$$M^{\mathrm{L}}_{\alpha\beta} = \int_{V^{\mathrm{L}}} (\Phi^{\mathrm{L}}_\alpha \Phi^{\mathrm{L}}_\beta)\,\mathrm{d}V,$$

$$M^{n+1}_{\alpha\beta} = \int_{V^{n+1}} (\Phi^{n+1}_\alpha \Phi^{n+1}_\beta)\,\mathrm{d}V,$$

$$H^{\mathrm{L}}_{\alpha i\beta} = \int_{V^{\mathrm{L}}} (\Phi^{\mathrm{L}}_{\alpha,i} \Phi^{\mathrm{L}}_\beta)\,\mathrm{d}V,$$

$$H^{n+1}_{\alpha i\beta} = \int_{V^{n+1}} (\Phi^{n+1}_{\alpha,i} \Phi^{n+1}_\beta)\,\mathrm{d}V,$$

$$K^n_{\alpha\beta\gamma j} = \int_{V^n} (\Phi^n_\alpha \Phi^n_{\beta,j} \Phi^n_\gamma)\,\mathrm{d}V,$$

$$A^{\mathrm{L}}_{\alpha\beta} = \int_{V^{\mathrm{L}}} (\Phi^{\mathrm{L}}_{\alpha,i} \Phi^{\mathrm{L}}_{\beta,i})\,\mathrm{d}V,$$

$$A^{n+1}_{\alpha\beta} = \int_{V^{n+1}} (\Phi^{n+1}_{\alpha,i} \Phi^{n+1}_{\beta,i})\,\mathrm{d}V,$$

$$N^n_\alpha = \int_{V^n} (\Phi^n_\alpha)\,\mathrm{d}V,$$

$$\hat{\Omega}^{\mathrm{L}}_{\alpha i} = \int_{S^{\mathrm{L}}} \{\Phi^{\mathrm{L}} \nu (v^{\mathrm{L}}_{i,j} + v^{\mathrm{L}}_{j,i}) n_j\}\,\mathrm{d}S,$$

$$\hat{\Sigma}^{\mathrm{L}}_\alpha = \int_{S^{\mathrm{L}}} (\Phi^{\mathrm{L}}_\alpha p^{\mathrm{L}}_{,i} n_i)\,\mathrm{d}S,$$

$$\hat{\Sigma}^{n+1}_\alpha \int_{s^{n+1}} (\Phi^{n+1}_\alpha p^{n+1}_{,i} n_j)\,\mathrm{d}S,$$

$$S^m_{\alpha i\beta i} = \nu \left\{ \int_{V^n} (\Phi^n_{\alpha,k} \Phi^n_{\beta,k}) \delta_{ij}\,\mathrm{d}V + \int_{V^n} (\Phi^n_{\alpha,i} \Phi^n_{\beta,j})\,\mathrm{d}V \right\}.$$

In equations (64)–(70), $\bar{M}_{\alpha\beta}$ means the lumped mass matrix obtained simply by summing across each row of the consistent mass matrix $M_{\alpha\beta}$, and placing the results on the diagonal.

STABILITY ANALYSIS

In this section the stability criterion is analysed for the one-dimensional advection–diffusion equation. The conditions for numerical stability of the equations are provided, resulting from the linear spatial discretization combined with a first-order Euler scheme as an explicit time integration technique. It is generally known that the explicit method is conditionally stable, and that the time increment Δt has to satisfy the following condition:[27]

$$0 < \Delta t \leqslant \Delta t_0, \tag{71}$$

where Δt_0 is the limiting value of Δt and depends on various factors, such as the coefficient of kinematic viscosity and mesh size.

The Navier–Stokes equation is a generalization of the simpler convection–diffusion equation and, in the one-dimensional case, it reduces to

$$\frac{\partial v}{\partial t} + U\frac{\partial v}{\partial x} - \nu\frac{\partial^2 v}{\partial x^2} = 0, \tag{72}$$

where v is the velocity and U, ν are a reference velocity and the kinematic viscosity coefficient, respectively, and the latter two are assumed constant. Assume an initial condition in the form of a spatial Fourier component:

$$v(x,0) = v_n \exp(\mathrm{i}\sigma_n x). \tag{73}$$

The exact solution of the partial differential equation (72) is

$$v = \sum_{n=-\infty}^{\infty} v_n \exp\{\mathrm{i}(\sigma_n x + \beta_n t)\}, \tag{74}$$

where β_n is the frequency of the nth component, σ_n is the spatial frequency and $\mathrm{i} = (-1)^{1/2}$. Because equation (72) is linear, it is necessary to consider only one component of the summation represented by (74),

$$v = v_n \exp\{\mathrm{i}(\sigma_n x + \beta_n t)\}. \tag{75}$$

To determine the analytic relationship between the spatial frequency and the frequency of the nth component, equation (75) is introduced into equation (72) to give

$$\beta_n + U\sigma_n - \mathrm{i}\nu\sigma_n^2 = 0, \tag{76}$$

or, for the frequency β_n as a function of σ_n,

$$\beta_n = \sigma_n(\mathrm{i}\nu\sigma_n^2 - U), \tag{77}$$

or,

$$\begin{aligned} -\mathrm{i}\beta_n &= -(\nu\sigma_n^2 + \mathrm{i}\sigma_n U) \\ &= -(\delta + \mathrm{i}\omega) \\ &= \lambda. \end{aligned} \tag{78}$$

By definition, $\delta = \nu\sigma_n^2$ is the exact damping parameter and $\omega = \sigma_n U$ is the exact frequency. Therefore, equation (75) can be rewritten in the following form:

$$v = v_n \exp(\mathrm{i}\sigma_n x - \nu t). \tag{79}$$

For a uniform mesh of piecewise linear finite elements, the Galerkin formulation provides spatially discrete equations for the nodal values $v_n(t)$, $n = 1, 2, \ldots$. The equations are

$$\dot{v}_n + r(\dot{v}_{n+1} - 2\dot{v}_n + \dot{v}_{n-1}) + \frac{U}{2h}(v_{n+1} - v_{n-1}) - \frac{\nu}{h^2}(v_{n+1} - 2v_n + v_{n-1}) = 0, \tag{80}$$

where h is the dimension of the linear elements. In the case of diagonal mass representation $r = 0$ and in the case of a consistent mass matrix form $r = \frac{1}{6}$. In the present case equation (80) reduces to

$$\dot{v}_n + \frac{U}{2h}(v_{n+1} - v_{n-1}) - \frac{\nu}{h^2}(v_{n+1} - 2v_n + v_{n-1}) = 0. \tag{81}$$

The solution of the semi-descrete equation (81) can be interpreted as solution of the simple ordinary differential equation

$$\frac{\mathrm{d}v}{\mathrm{d}t} + \bar{\lambda} v = 0, \tag{82}$$

where the semi-discrete response variable $\bar{\lambda} = \bar{\delta} + \mathrm{i}\bar{\omega}$ depends on the considered spatial approximation. Using Euler's first order explicit scheme, equation (82) can be approximated as follows:

$$\begin{aligned} v_{n+1} &= v_n - \Delta t\, \bar{\lambda} v_n \\ &= (1 - \bar{\lambda}\Delta t) v_n. \end{aligned} \tag{83}$$

The amplification factor for this problem is

$$\left| \frac{v_{n+1}}{v_n} \right| = |G| = |1 - \bar{\lambda}\Delta t|. \tag{84}$$

For stability it is necessary to have

$$|1 - \bar{\lambda}\Delta t| \leqslant 1, \tag{85}$$

or

$$\Delta t^2(\bar{\delta}^2 + \bar{\omega}^2) \leqslant 2\bar{\delta}\Delta t. \tag{86}$$

From equation (86) the stability condition becomes

$$\Delta t \leqslant \frac{2\bar{\delta}}{\bar{\delta}^2 + \bar{\omega}^2}. \tag{87}$$

SOLITARY WAVE PROPAGATION

The analysis for the propagation of a solitary wave is important for the design of breakwaters or sea walls, and other offshore structures. The phenomenon of a solitary wave travelling in a rectangular channel of uniform depth was first reported by John Scott Russell in 1834. Russell defined the solitary wave as a single elevation above the surrounding undisturbed water level, neither followed nor preceded by any other elevation or depression of the surface, producing a definite transport in the direction of wave propagation only, and travelling without change of shape and with essentially constant velocity throughout the observable time of travel. Analytical studies for this problem have been carried out by many investigators.[28–30] Laitone's approximations of a solitary wave are frequently used for comparative study; in these approximations velocity, pressure and free surface elevation can be written in the following forms:

$$v_1 = \sqrt{(gd)}\frac{H}{d}\operatorname{sech}^2\left[\sqrt{\left(\frac{3}{4}\frac{H}{d^3}\right)}(x_1 - ct)\right], \tag{88}$$

$$v_2 = \sqrt{(3gd)}\left(\frac{H}{d}\right)^{3/2}\left(\frac{X_2}{d}\right)\operatorname{sech}^2\left[\sqrt{\left(\frac{3}{4}\frac{H}{d^3}\right)}(x_1 - ct)\right]\tanh\left[\sqrt{\left(\frac{3}{4}\frac{H}{d^3}\right)}(x_1 - ct)\right], \tag{89}$$

$$\eta = d + H\operatorname{sech}^2\left[\sqrt{\left(\frac{3}{4}\frac{\mathrm{H}}{d^3}\right)}(x_1 - ct)\right], \tag{90}$$

$$p = \rho g(\eta - x_2), \tag{91}$$

where

$$c = \sqrt{\left[gd\left(1 + \frac{1}{2}\frac{H}{d}\right)\right]}, \tag{92}$$

in which H and d are the initial wave height and still water depth, respectively. In theory, Laitone's formula holds for an infinitely long channel only. Because the computations must be done in a finite domain and the fluid at a distance from the wave crest is essentially still, it is desirable to define a finite, practical length of the solitary wave. The main consideration is that the two vertical walls which constitute the boundaries of the computation region should be far enough from the initial wave crest so that the motion of a solitary wave into the still water in front of a vertical wall can be closely approximated. For this purpose the effective wavelength L was obtained by taking $L/2$ equal to the distance from the wave crest to the section where $\eta = 0{\cdot}01\,H$ according to Laitone's formula; thus

$$\frac{L}{d} = 6{\cdot}90\left(\frac{d}{H}\right)^{1/2}. \tag{93}$$

Considering $H/d = 0{\cdot}2$, the value of $L/2$ is given by $8d$ by equation (93). Thus, the two vertical walls were located $16d$ away from the initial crest. The definition sketch is shown in Figure 2. The initial condition for this problem is illustrated in Figure 3. The still water depth d is 10 units, the wave height H is 2·0 units and the horizontal length of the channel is $16d = 160{\cdot}0$ units. For computation, the density is assumed to be constant, the gravity acceleration is taken as $g = 9{\cdot}8$ units and the time increment $\Delta t = 0{\cdot}02$ time units is used. The finite element idealization, velocity and pressure contours at the initial stage are shown in Figure 3. Starting from the initial condition, the behaviour of the solitary wave can be computed. Computed wave profile, velocity and pressure at elapsed times 7·7 units, 15·0 units and 30·0 units are shown in Figures 4–6. The time when the wave crest arrives at the right hand vertical wall from the centre of the channel is 7·7 time units, which is close to Laitone's result.

The run-up height of a solitary wave on a vertical wall R can be obtained by Laitone's approximation:

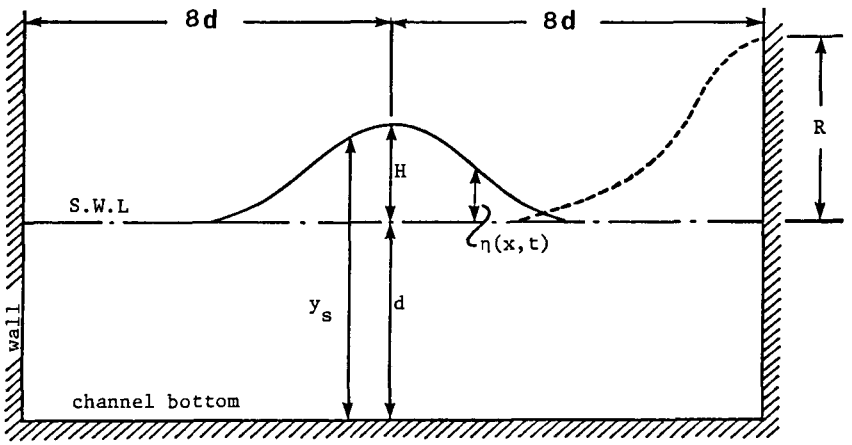

Figure 2. Problem definition for solitary wave propagation

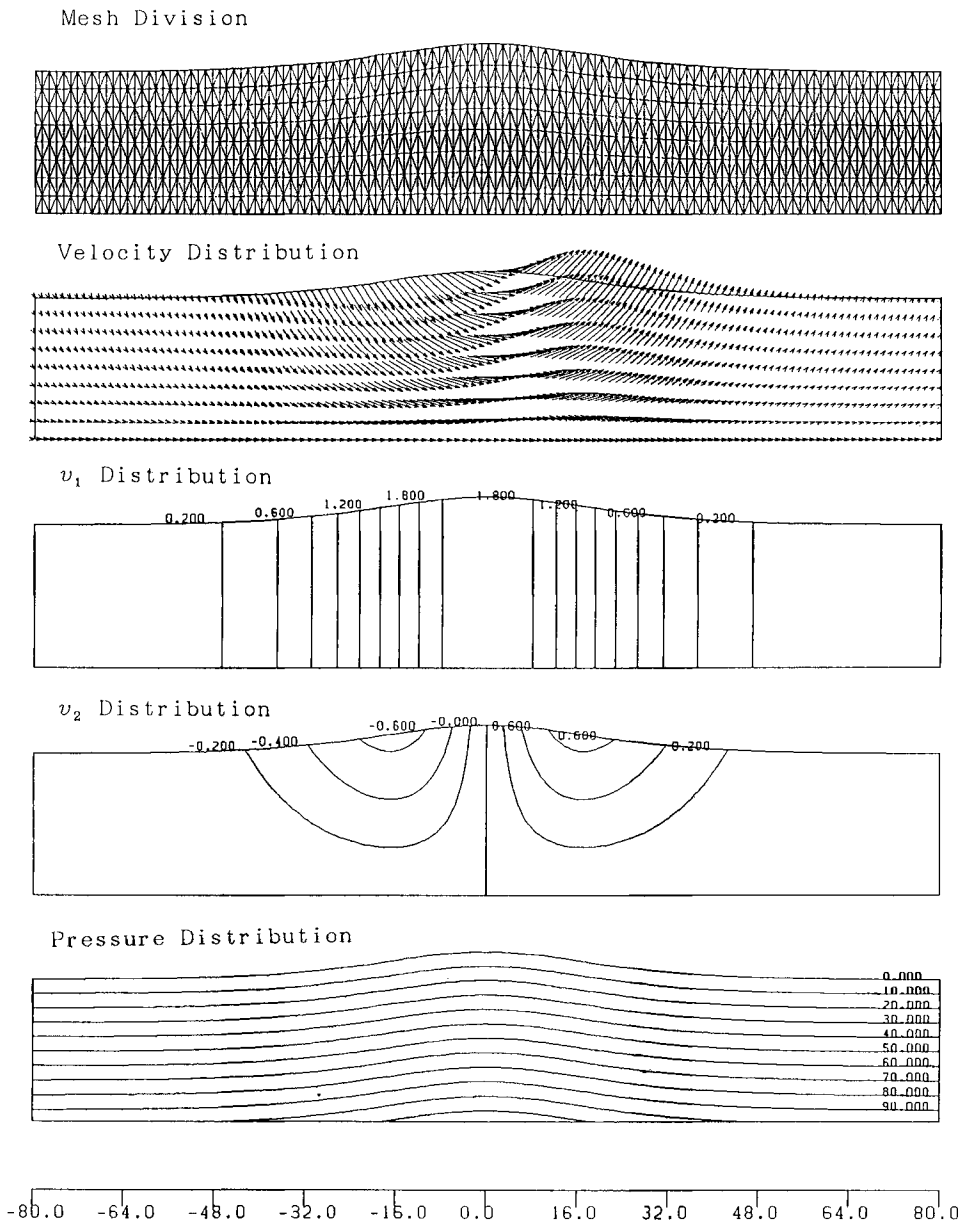

Figure 3. Initial conditions

$$\frac{R}{d}=2\left(\frac{H}{d}\right)+\frac{1}{2}\left(\frac{H^2}{d}\right). \tag{94}$$

Using $H/d=0{\cdot}2$, R is 4·2 units in this computation, whereas the computed result is $R=4{\cdot}48$ units. This clearly shows that the present method is not affected by any artificial damping effect. The pressure p is almost equal to hydrostatic pressure, and this result is reasonably well in agreement with practical behaviour. Thus the successful application of the present approach to

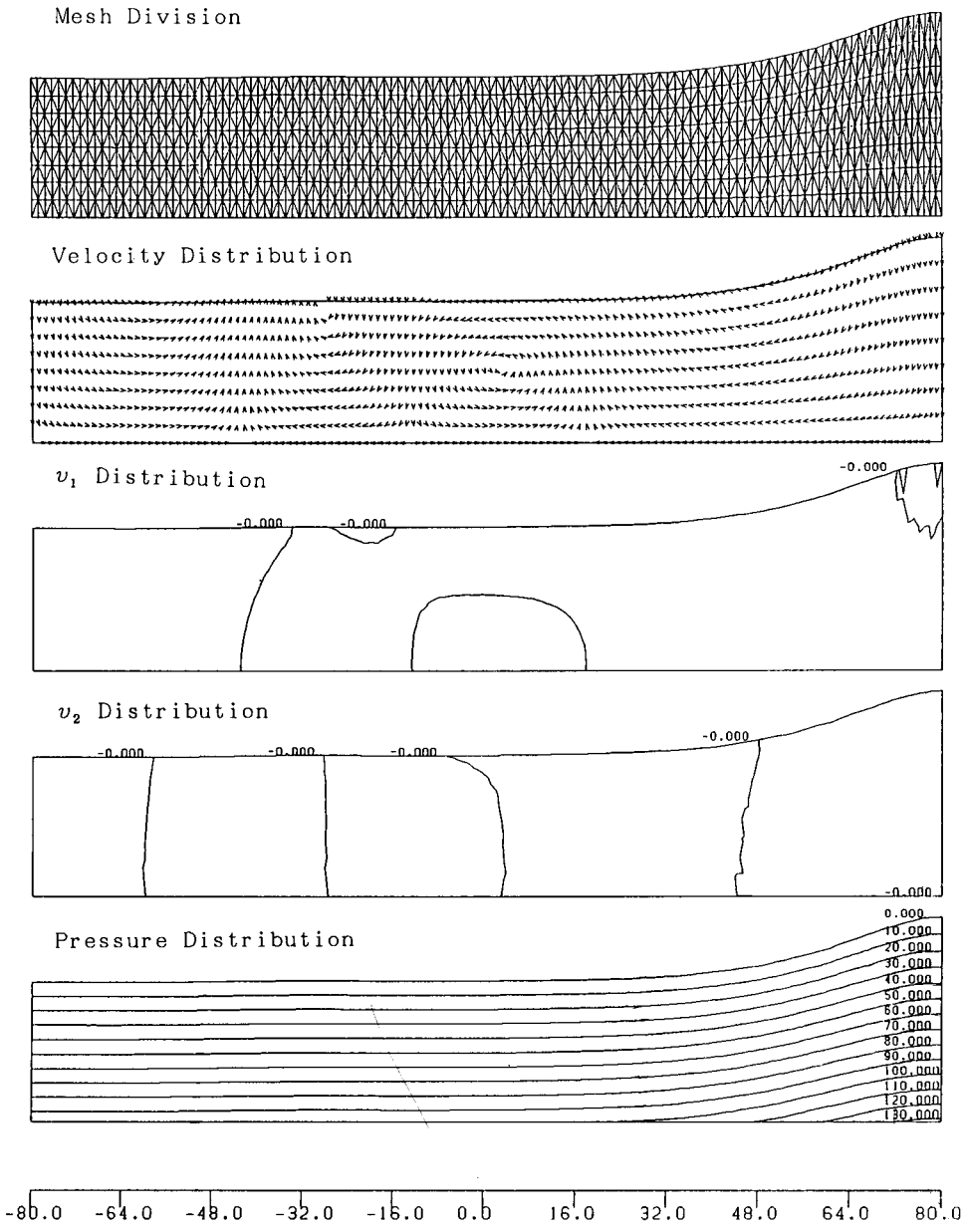

Figure 4. Computed results at time $t = 7{\cdot}7$

the run-up of a solitary wave indicates the possibility of employing the same technique to attack a wide variety of water wave problems. This extension will prove to be most valuable in problems where analytic methods are difficult, if not impossible.

LARGE AMPLITUDE SLOSHING DYNAMICS

To show the adaptability of the present arbitrary Lagrangian–Eulerian finite element method,

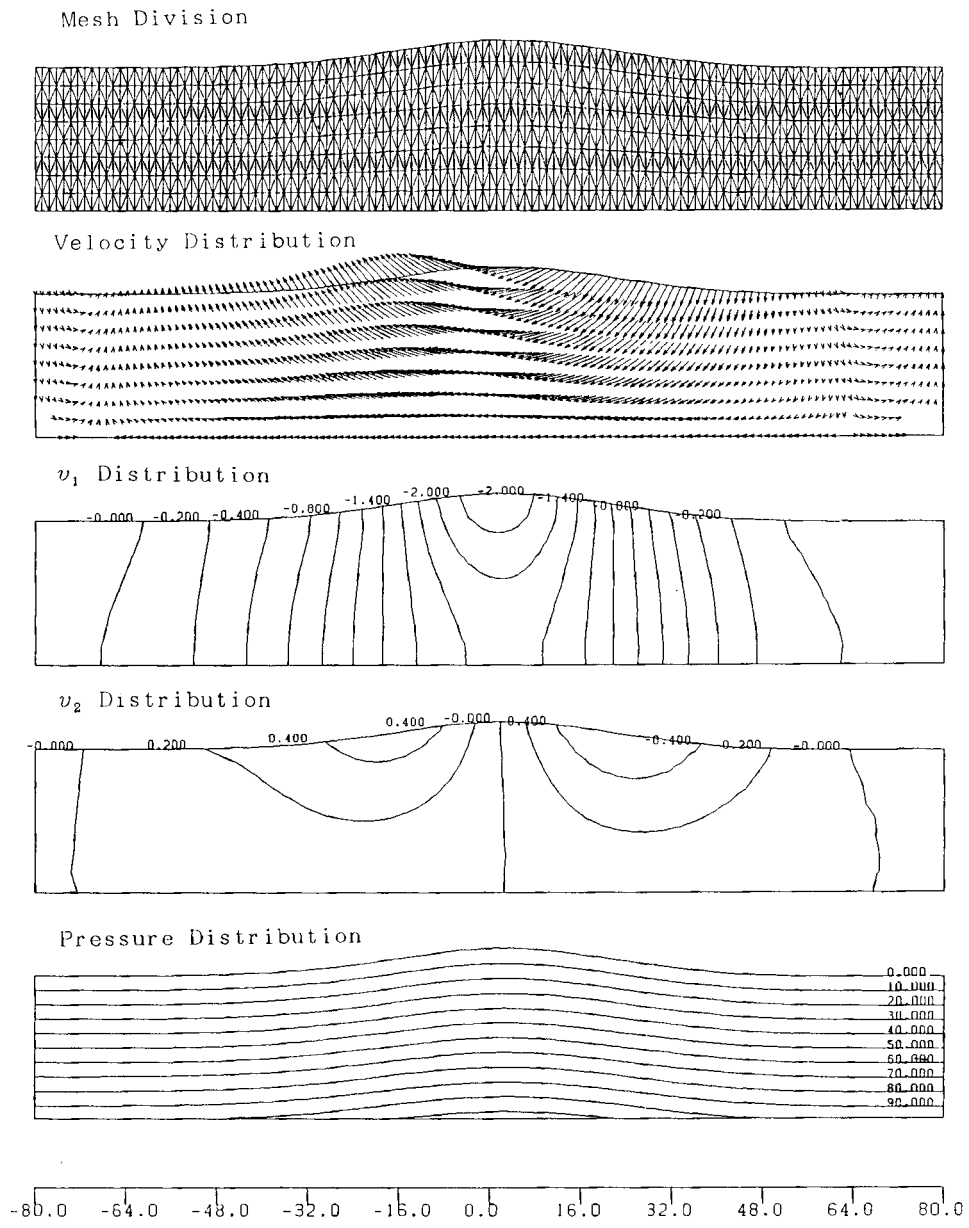

Figure 5. Computed results at time $t = 15{\cdot}0$

the analysis of a case involving large amplitude sloshing dynamics in a rectangular tank with constant or varying water depth has been carried out. The physical problem is pictured in Figure 7. In this problem, a fluid sloshes in a rectangular container. At first, the analysis is carried out for the rectangular tank with constant depth whose width (L) is 4·8 units and the height of the original free surface (D) is 4·0 units. In this case, the fluid, initially at rest in a rectangular tank, is impulsively set in motion by a cosine pressure pulse at the free surface. The pressure pulse is given by

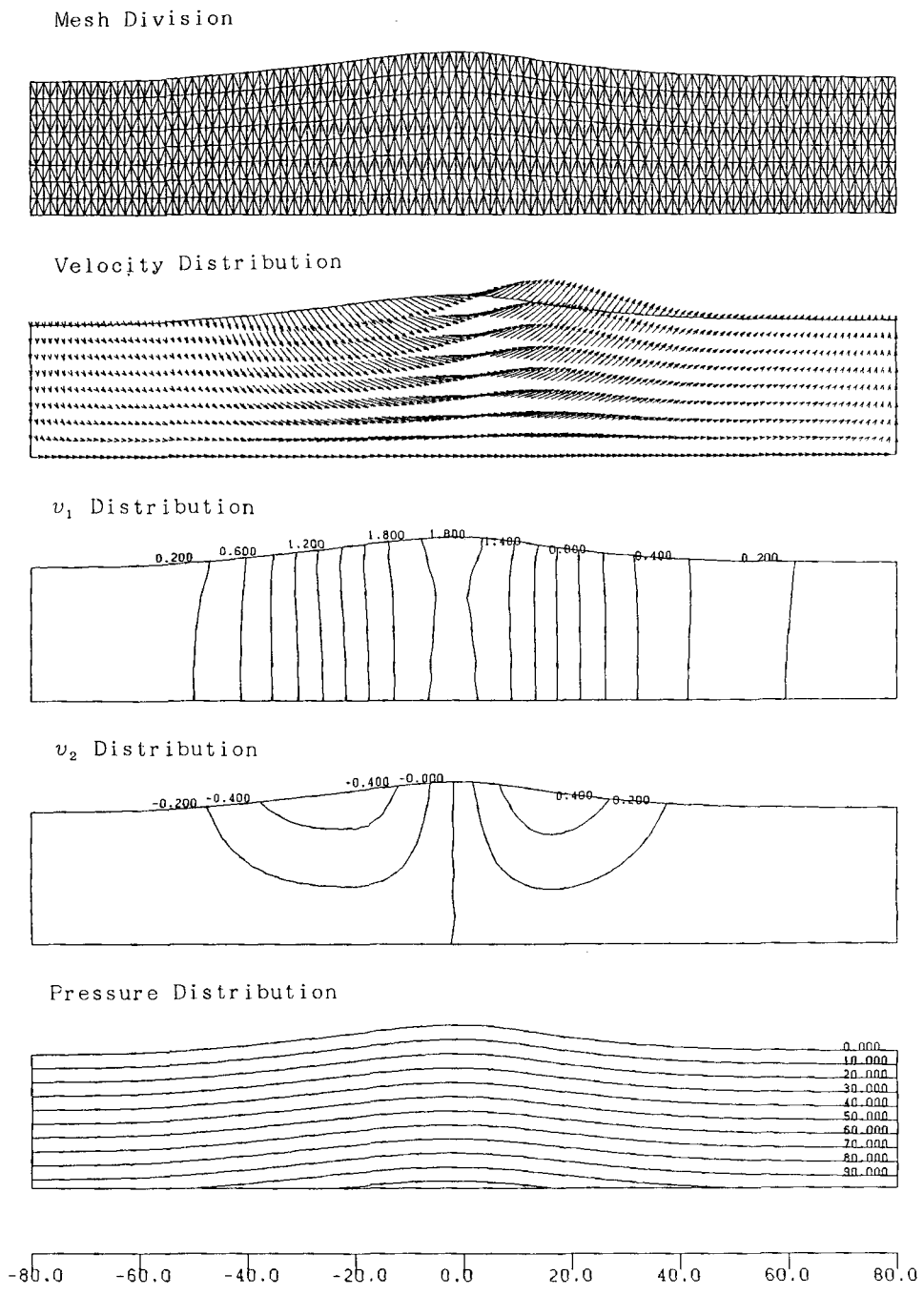

Figure 6. Computed results at time $t = 30{\cdot}0$

$$p(t) = A\delta(t)\cos(kx_1), \tag{95}$$

where $\delta(t)$ is the Dirac delta function. A gravity acceleration of one unit acts downwards and the amplitude of the impulsive motion is assumed to be unity.

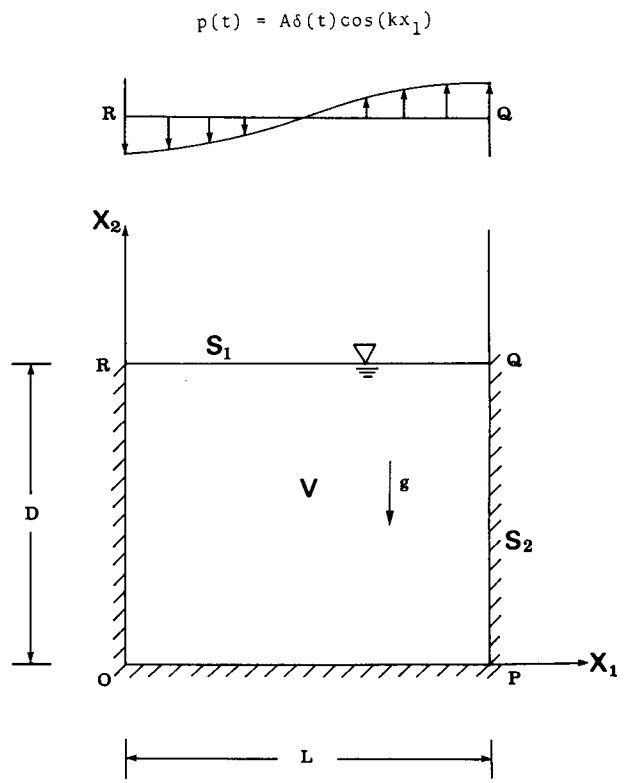

Figure 7. Problem definition for sloshing dynamics

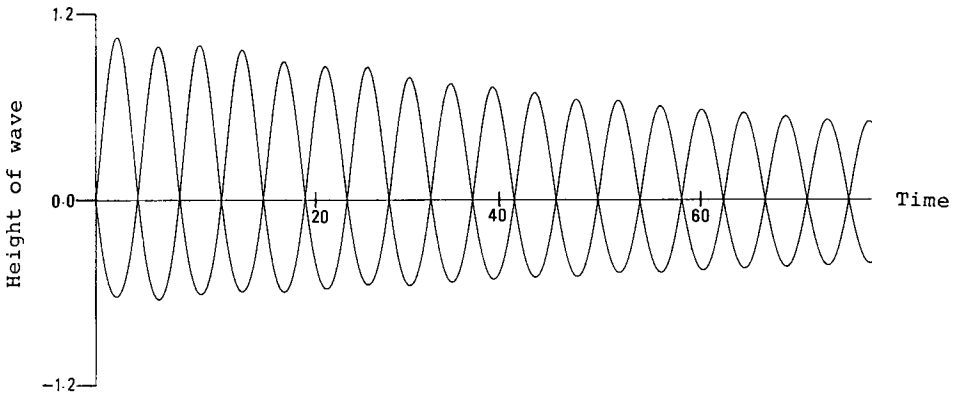

Figure 8. Amplitudes of spike and bubble as functions of time for sloshing dynamics

The calculation started with a half-wave impulsive loading of the free surface as given in equation (95). The amplitudes of the spikes and bubbles as functions of time through many complete periods of oscillation are shown in Figure 8. One of the principal manifestations of non-linearity is seen in the enhanced amplitude of the spike side and the reduced amplitude of the bubble. The decreased frequency is indicated by shifts in both the time of maximum amplitude and the times for return to zero amplitude.

The computation of the non-linear oscillation in a tank with varying water depth has also

been carried out. A schematic view of the tank and the boundary conditions are shown in Figure 9. The bottom width of the tank is 10.0 units and the depth is 10.0 units. A gravity acceleration of one unit acts downwards and the amplitude of the impulsive motion is assumed to be 10·0 units. The calculation was performed with viscosity 0·01 units. Figures 10–14 show a sequence of mesh configurations at a sequence of times. In this calculation the rezoning is performed at every 1000 time levels. From the results, it can be seen clearly that the rezoning process makes a finer mesh where the speed of the fluid particle is high and a coarser mesh where the speed is low. The non-linear effects are also cearly shown in all these computed results by noting the movement of the nodal points in the whole region. $\Delta t = 0{\cdot}0025$ units was used and a stable calculation was obtained.

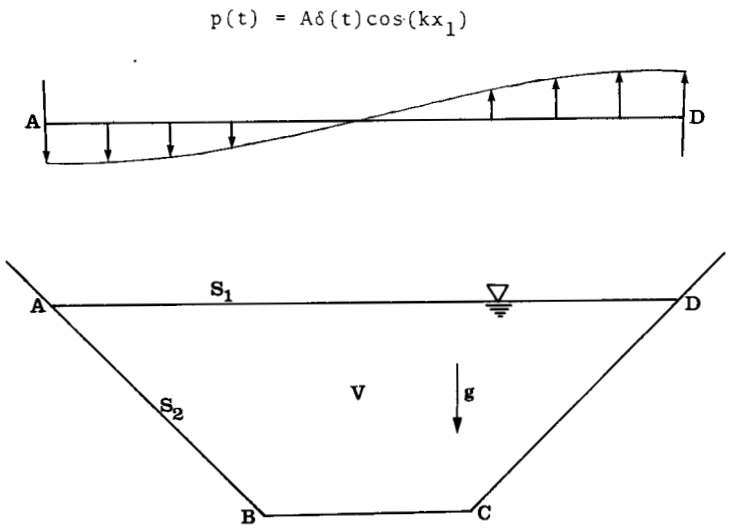

Figure 9. Schematic view and boundary conditions

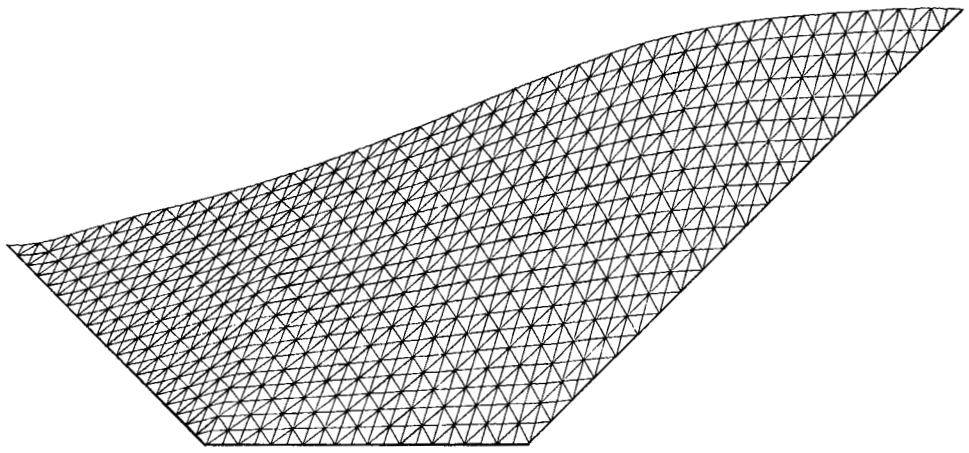

Figure 10. Computed mesh diagram at time $t = 5{\cdot}0$

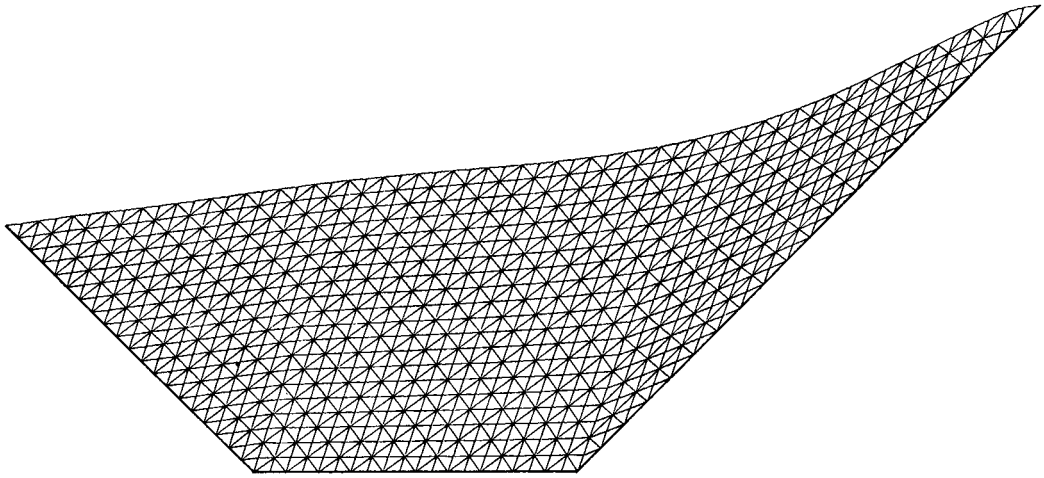

Figure 11. Computed mesh diagram at time $t = 10{\cdot}0$

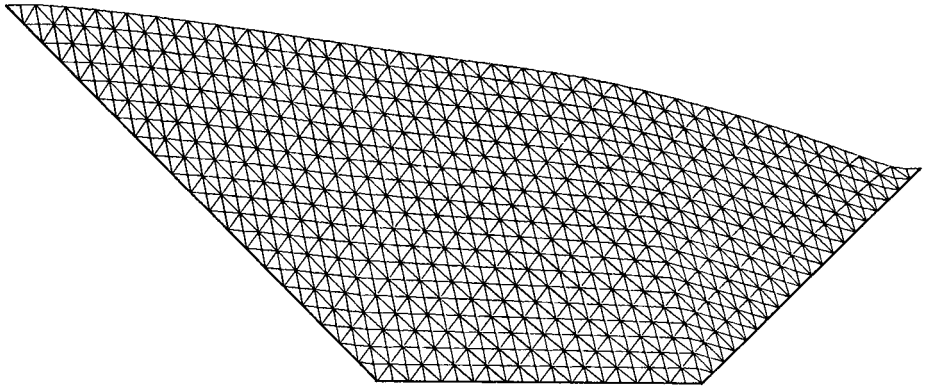

Figure 12. Computed mesh diagram at time $t = 15{\cdot}0$

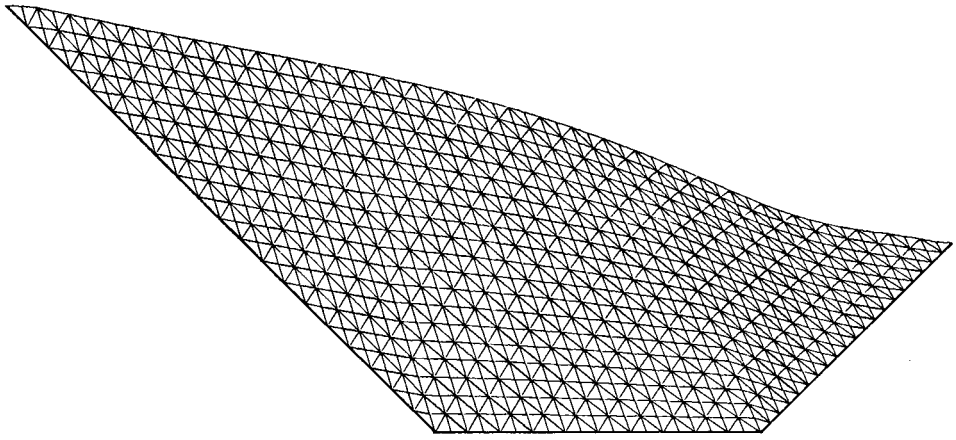

Figure 13. Computed mesh diagram at time $t = 20{\cdot}0$

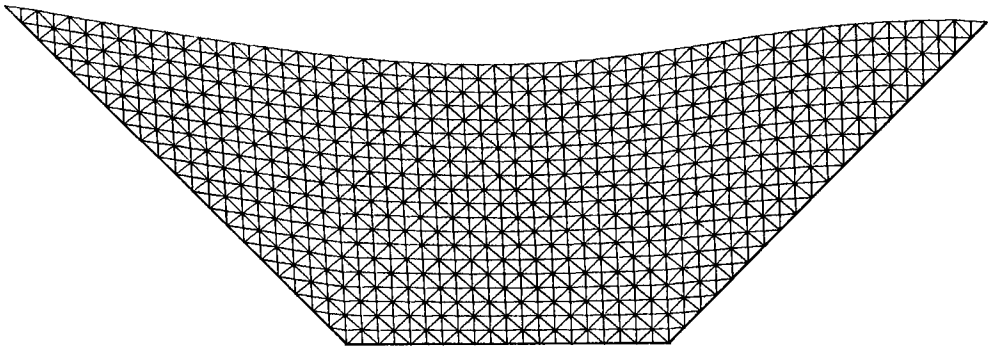

Figure 14. Computed mesh diagram at time $t = 25{\cdot}0$

CONCLUDING REMARKS

The conclusions from the work described in this paper are:

1. The arbitrary Lagrangian–Eulerian (ALE) technique has been presented as a simple and efficient means of numerically treating free boundaries embedded in a calculational mesh of arbitrary Lagrangian–Eulerian elements.
2. This new algorithm is particularly useful because it uses a minimum of stored information, treats complicated free boundaries automatically, and could be extended to three dimensions.
3. The ALE technique was described in detail, as it has been used to follow free surfaces in an incompressible hydrodynamics code. The advantages of the ALE method include its ability to resolve arbitrary confining boundaries, to have variable zoning for purposes of obtaining optimum resolution and to be almost Lagrangian for improved accuracy in problems where fully Lagrangian calculations are not possible. Sample calculations with the developed new scheme show that it works well for a wide range of complicated problems.
4. Since the ALE computing grid can always be rezoned to its original location, it can be used for purely Eulerian calculations where boundaries can then be treated as rigid or as input and output walls.
5. The present computing technique is not affected by the spurious phenomenon of spatial oscillations of the pressure—the so-called chequerboard splitting encountered in some other studies.
6. Because of the highly stable and convergent nature of this method, even for very large time steps, it will prove to be a useful tool in the solution not only of free boundary flow, but generally of time-dependent fluid dynamical problems.

ACKNOWLEDGEMENTS

The authors wish to thank Dr. T. Nakayama of Chuo University, for his interest, encouragement, and many helpful discussions. The computations have been carried out using the FACOM M170F of Chuo University and the HITAC M680H of the University of Tokyo. The use of these computer facilities is also gratefully acknowledged.

REFERENCES

1. F. H. Harlow and J. E. Welch, 'Numerical calculation of time-dependent viscous incompressible flow of fluid with free surface', *Phys. Fluids*, **8**, 2189–2189 (1965).

2. A. A. Amsden and F. H. Harlow, 'A simplified MAC technique for incompressible fluid flow calculations', *J. Comp. Phys.*, **6**, 322–325 (1970).
3. R. K.-C. Chan and R. L. Street, 'A computer study of finite-amplitude water waves', *J. Comp. Phys.*, **6**, 68–94 (1970).
4. R. E. Nickell, R. I. Tanner and B. Caswell, 'The solution of viscous incompressible jet and free-surface flows using finite element method', *J. Fluid. Mech.*, **65**, 189–206 (1974).
5. F. M. Orr and L. E. Scriven, 'Rimming flow: numerical simulation of steady, viscous, free-surface flow with surface tension', *J. Fluid. Mech.*, **84**, 145–165 (1978).
6. B. J. Omodei, 'Computer solutions of a plane Newtonian jet with free surface tension', *Comp. Fluids*, **7**, 79–96 (1986).
7. L. C. Wellford and T. H. Ganaba, 'A finite element method with hybrid Lagrange line for fluid mechanics problems involving large free surface motion', *Int. j. numer. methods eng.*, **17**, 1201–1231 (1981).
8. C. S. Frederiksen and A. M. Watts, 'Finite element method for time-dependent incompressible free surface flow', *J. Comp. Phys.*, **39**, 282–304 (1981).
9. M. Kawahara and T. Miwa, 'Finite element analysis of wave motion', *Int. j. numer. methods eng.*, **20**, 1193–1210 (1984).
10. K. Washizu, T. Nakayama and M. Ikegawa, 'Application of the finite element method to some free surface fluid problems', in W. G. Gray *et al.*, *Finite Elements in Water Resources*, Pentech Press, London, 1978, pp. 247–266.
11. P. Bach and O. Hassager, 'An algorithm for the use of the Lagrangian specification in Newtonian fluid mechanics and applications to free-surface flow', *J. Fluid Mech.*, **152**, 173–190 (1985).
12. M. Kawahara, B. Ramaswamy and A. Anjyu, 'Lagrangian finite element method for nonlinear free surface motions', *Proc. Int. Conf. Finite Elements in Computational Mechanics*, Bombay, 1985, pp. 579–588.
13. M. Kawahara, B. Ramaswamy and A. Anjyu, 'Lagrangian finite element method for wave motion using velocity correction method', *Journal of JSCE*, No. 369/II-5, 203–211 (1986).
14. B. Ramaswamy, M. Kawahara and T. Nakayama, 'Lagrangian finite element method for the analysis of two-dimensional sloshing problems', *Int. j. numer. methods fluids*, **6**, 659–670 (1986).
15. B. Ramaswamy and M. Kawahara, 'Lagrangian finite element analysis applied to viscous free surface fluid flow', *Int. j. numer. methods fluids*, **7**, 953–984 (1987).
16. A. A. Amsden and C. W. Hirt, 'YAQUI: an arbitrary Lagrangian–Eulerian computer program for fluid at all speeds', *Los Alamos Scientific Laboratory Report, LA-5100*, 1973.
17. C. W. Hirt, A. A. Amsden and J. L. Cook, 'An arbitrary Lagrangian–Eulerian computing method for all flow speeds', *J. Comp. Phys.*, **14**, 227–253 (1974).
18. R. K.-C. Chan, 'A generalized arbitrary Lagrangian–Eulerian method for incompressible flows with sharp interfaces', *J. Comp. Phys.*, **17**, 311–331 (1975).
19. W. E. Pracht, 'Calculating three-dimensional fluid flows at all speeds with an Eulerian–Lagrangian computing mesh', *J. Comp. Phys.*, **17**, 132–159 (1975).
20. J. Donea, S. Giuliani and J. P. Halleux, 'An arbitrary Lagrangian–Eulerian finite element method for transient dynamic fluid–structure interactions', *Comp. Meth. Appl. Mech. Eng.*, **33**, 689–723 (1982).
21. J. Donea, 'Arbitrary Lagrangian–Eulerian finite element methods', in T. B. Belytschko and T. J. R. Hughes (eds), *Computational Methods for Transient Analysis*, 1983, pp. 474–516.
22. T. B. Belytschko and J. M. Kennedy, 'Computer models for subassembly simulation', *Nuc. Eng. Design*, **49**, 17–38 (1978).
23. T. B. Belytschko and D. P. Flanagan, 'Finite element methods with user-controlled meshes for fluid–structure interaction', *Comput. Meth. Appl. Mech. Eng.*, **33**, 669–688 (1982).
24. T. J. R. Hughes, W. K. Liu and T. Zimmerman, 'Lagrangian–Eulerian finite element formulation for incompressible viscous flow', *Comput. Meth. Appl. Mech. Eng.*, **29**, 329–349 (1981).
25. W. K. Liu and D. C. Ma, 'Computer implementation aspects for fluid–structure interaction problems', *Comput. Meth. Appl. Mech. Eng.*, **31**, 129–148 (1982).
26. B. Ramaswamy and M. Kawahara, 'Arbitrary Lagrangian–Eulerian finite element method for the analysis of fluid flow with free surface', *Proc. Int. Conf. Computational Mechanics*, Tokyo, 1986, pp. VII103–108.
27. P. J. Roache, *Computational Fluid Dynamics*, Hermosa Publishers, 1972.
28. E. V. Laitone, 'The second approximation to conoidal and solitary waves', *J. Fluid. Mech.*, **9**, 430–444 (1960).
29. R. Grimshaw, 'The solitary wave in water of variable depth', *J. Fluid. Mech.*, **46**, 611–622 (1971).
30. J. Fenton, 'A ninth-order solution for the solitary waves', *J. Fluid. Mech.*, **53**, 257–271 (1972).